BNL-80069-2008-JA

HYDROGEN BONDING INTERACTION OF MOLECULAR COMPLEXES AND CLUSTERS OF AEROSOL NUCLEATION PRECURSORS

Zhao, J., Zhang, R., and McGraw, R.

Submitted to
Journal of Chemical Physics

March 2008

Environmental Sciences Department/Atmospheric Sciences Division

Brookhaven National Laboratory
P.O. Box 5000
Upton, NY 11973-5000
www.bnl.gov

Notice: This manuscript has been authored by employees of Brookhaven Science Associates, LLC under Contract No. DE-AC02-98CH10886 with the U.S. Department of Energy. The publisher by accepting the manuscript for publication acknowledges that the United States Government retains a non-exclusive, paid-up, irrevocable, world-wide license to publish or reproduce the published form of this manuscript, or allow others to do so, for United States Government purposes.

This preprint is intended for publication in a journal or proceedings. Since changes may be made before publication, it may not be cited or reproduced without the author's permission.

DISCLAIMER

This report was prepared as an account of work sponsored by an agency of the United States Government. Neither the United States Government nor any agency thereof, nor any of their employees, nor any of their contractors, subcontractors, or their employees, makes any warranty, express or implied, or assumes any legal liability or responsibility for the accuracy, completeness, or any third party's use or the results of such use of any information, apparatus, product, or process disclosed, or represents that its use would not infringe privately owned rights. Reference herein to any specific commercial product, process, or service by trade name, trademark, manufacturer, or otherwise, does not necessarily constitute or imply its endorsement, recommendation, or favoring by the United States Government or any agency thereof or its contractors or subcontractors. The views and opinions of authors expressed herein do not necessarily state or reflect those of the United States Government or any agency thereof.

Printed on recycled paper

Hydrogen Bonding Interaction of Molecular Complexes and Clusters of Aerosol Nucleation Precursors

Jun Zhao[1] and Renyi Zhang*

Department of Atmospheric Sciences and Department of Chemistry, Texas A&M University, College Station, TX 77843

Robert McGraw

Atmospheric Sciences Division, Brookhaven National Laboratory, P.O. Box 5000, Upton, NY 11973

Abstract. Molecular complexes and clusters bridge the gap between microscopic molecules and macroscopic freshly-formed nuclei in the atmosphere. The driving forces for the formation of these complexes and clusters are hydrogen bonding interactions, which are not well characterized. In this study, we performed quantum chemical calculations to elucidate the role of hydrogen bonding in complex and cluster formation of the atmospheric nucleating precursors (sulfuric acid, water, ammonia and organic acids). The results indicate that organic acid–sulfuric acid complexes bear a hydrogen bond pair with one strong and one medium-strength hydrogen bonding according to the bond length, bond angle and the contact distance of the hydrogen bonds, while the hydrogen bond pair in organic-ammonia is characterized by one medium-strength and one weak hydrogen bond interactions. The formation of the hydrogen bonds in organic acid–sulfuric acid complexes can be explained by the well-established resonance-assisted hydrogen bonding theory. The bonding energies of the organic acid–sulfuric acid complexes are ~20 kcal mol^{-1}, much (up to 7 kcal mol^{-1}) stronger than those of the corresponding organic acid-ammonia complexes. Topological analysis employing quantum theory of atoms in molecules (QTAIM) shows that the charge density and the Laplacian at bond critical points

(BCPs) of the hydrogen bonds of the organic acid–sulfuric acid (e.g. benzoic acid-sulfuric acid and cis-pinonic acid-sulfuric acid) are 0.07 and 0.16 au, respectively, which falls in the range or exceeds the range of one strong and one medium-strength hydrogen bonding criteria.

*Corresponding author

Prof. Renyi Zhang

Fax: 979-862-4466

Email: zhang@ariel.met.tamu.edu

[1] Now at The National Center for Atmospheric Research, Atmospheric Chemistry Division, Boulder, CO 80307

1. Introduction

New particle formation involving sulfuric acid as a principal atmospheric nucleating agent represents an important contributor of nucleation mode aerosols.[1] Field measurements have consistently shown that the contribution of sulfuric acid to the particle growth is substantially low during the nucleation events in various locations,[2,3] revealing that atmospheric new particles are essentially multi-components. Other likely nucleating precursors include the ubiquitous species NH_3 and organic compounds. Experimental study showed that the binary H_2SO_4–H_2O nucleation rates increased by up to several hundred folds in the presence of ppb to parts per million (ppm) levels of NH_3.[4,5] Furthermore, classic and kinetic nucleation models predict much higher enhancement of the nucleation rates (up to 30 orders of magnitude) in the presence of parts per trillion (ppt) levels of NH_3.[6-10] Field measurements have shown that atmospheric aerosol particles contain a substantial fraction of organic compounds.[1] Recent laboratory experiments have revealed that new particle formation in the binary sulfuric acid–water system is considerably enhanced in the presence of sub ppb levels of aromatic acids (e.g. benzoic acid, m-toluic acid, p-toluic acid).[11] However, the detailed roles of ammonia and organic compounds in new particle formation still remain largely unknown.

Although atmospheric aerosol nucleation has received intensive attention over decades and continuous progress has been made toward understanding the nucleation mechanism, new particle formation at a fundamental microscopic molecular level is still poorly understood. It is commonly recognized that molecular complex and pre-nucleation cluster formations are the initial stages for new particle formation. The molecular complexes and small clusters (usually smaller than 1 nm) containing up to several tens of molecules bridge the gap between single molecules and larger particles (e.g., larger than 3 nm) and play a vital role in the atmospheric

new particle formation process. Knowledge of the thermodynamic properties of these complexes and clusters is still very limited and the kinetic and dynamic molecular processes for formation of molecular aggregates remain largely unclear, hindering efforts to quantitatively predict atmospheric nucleation rates.

The driving forces for the formation of atmospheric molecular complexes are hydrogen bonding interactions, whose strength determines the thermodynamic stability of these complexes. Atmospherically relevant hydrogen-bonding complexes have been the subjects of numerous theoretical studies in recent years. The complexes and clusters of sulfuric acid with other species (e.g. water, ammonia and organics) are formed via hydrogen bonds of intermediate strength. Currently, the microscopic mechanism for atmospheric nucleation of sulfuric acid–water system is not known, but in general hydrogen bonding interaction is most likely the first step in this process, which determines the growth of clusters by condensation of sulfuric acid and other trace species. Due to the large affinity for water, gaseous sulfuric acid likely exists in hydrate form.[12,13] Previous quantum chemical calculations were focused on sulfuric acid hydrates $(H_2SO_4)_x(H_2O)_y$ (x=1–3, y=0–9) or sulfuric acid–ammonia and their hydrate clusters $(H_2SO_4)_x(H_2O)_y(NH_3)_z$ (x = 1–2, y = 0–5, z = 1). Kurdi and Kochanski performed ab initio calculations to investigate the monohydrate assuming rigid monomers, and the results indicate that the ionic complex is less stable than the neutral one.[14] Arstila et al. reported a density functional study of sulfuric acid mono-, di- and trihydrates and they found proton transfer is unlikely to occur in the mono- and dihydrate, while low energy barrier allows proton transfer to occur in the trihydrate,[15] consistent with the results by Bandy and Ianni,[16] who showed the existence of deprotonation in the clusters of $H_2SO_4(H_2O)_n$ (n = 3–7). Re et al. performed a molecular orbital study to explore the stability of the hydrated clusters containing up to 5 water

molecules and the results indicate the coexistence of both neutral and ionic structures under investigation.[17] Ding and Laasonen found that sulfuric acid can be partially deprotonated when three water molecules are present in the cluster and completely deprotonated in hydrated clusters containing eight or more water molecules.[18,19] For clusters containing two sulfuric acid molecules, the deprotonation of both acids will happen at the cluster containing five or more molecules of water, in contradiction to the results from Ianni and Bandy,[20] which show no deprotonation for clusters containing up to 6 water molecules. Al Natsheh et al. performed DFT calculations to investigate the molecular structures of the mono-, di-, and trihydrates of the sulfuric acid and the results imply that high dipole moments of these hydrates are important factors for the ultrafine particle formation in the atmosphere.[21] Recently, Kurten et al. revisited gas phase sulfuric acid monohydrate and ammonium hydrogen sulfate using different ab initio methods and density functional theory with various basis sets.[22] Their results indicated that different thermochemical parameters (e.g. reaction free energies) were predicted using different methods and basis sets partially due to the basis set superposition error (BSSE) and harmonic approximation. Ianni and Bandy presented a density functional study of clusters $NH_3 \cdot H_2SO_4 \cdot nH_2O$ (n = 0–5) and formation of the ion pair (NH_4^+ and HSO_4^-) is found to be energetically favored until the cluster contains 4 water molecules (n = 4).[23] Their results showed no role of NH_3 in new particle formation. In contrast, another DFT calculation showed that the $NH_3 \cdot H_2SO_4$ exists as the ion pair NH_4^+ and HSO_4^- in the presence of one or two water molecules.[24] Another recent density functional study indicated that ammonia is bonded much more strongly to the sulfuric acid–water clusters than water, implying that the ammonia may play a role in new particle formation.[25]

From the microscopic molecular point of view, how organic compounds participate in nucleation process remains an open question. Stable carboxylic acid dimers have been determined experimentally and theoretically.[26-30] It has been speculated that formation of stable dimers between carboxylic acids might be the first step in the new particle formation for the ozonolysis of pinenes.[31,32] Recent quantum chemical calculations indicate that formation of the unusually stable aromatic acid–sulfuric acid complex likely reduces the nucleation barrier and hence is responsible for the observed enhancement of the binary H_2SO_4–H_2O nucleation in the presence of sub ppb levels of organic acids.[11,33,34] Very recently, Nadykto and Yu performed quantum chemical calculations to investigate the thermodynamic stability of the hydrogen-bonded complexes of small carboxylic acids (e.g. formic and acetic acid) with free and hydrated sulfuric acid, and with ammonia.[30] The results indicate that both organic acids and ammonia may have efficiently stabilizing effects on the binary H_2SO_4–H_2O clusters and the organic acids can interact actively with ammonia.

In this study, we report density functional and ab initio molecular orbital study on the molecular complexes of atmospheric aerosol nucleating precursors (e.g. sulfuric acid, organic acids, water and ammonia). The optimized geometries of the complexes and clusters were determined using density functional theory, and the energies were calculated for each stationary point using MP2 and CCSD(T) theories with various basis sets. In addition, we also employed quantum theory of atoms in molecules (QTAIM) to elucidate the nature of the hydrogen bonds of these complexes and clusters and reveal their roles in new particle formation.[35]

2. Theoretical Methods

Ab initio orbital molecular calculations were performed on an SGI Altix 3700 supercomputer using the Gaussian 03 software package.[36] All the species were treated with the

restricted Hartree-Fock (RHF) formulation. Geometry optimization for complexes and their monomers was executed using Becke's three parameter hybrid method employing the LYP correction function (B3LYP) in conjunction with the split valence polarized basis set 6-31G(d,p). Harmonic vibrational frequency calculations were made using B3LYP/6-31G(d,p) to confirm the energy minima for all the structures of the relevant complex and monomers. The IR spectra for the complexes were obtained from the frequency calculations. The optimized structures were then employed in single-point energy calculations using frozen core second-order Møller-Plesset perturbation theory (MP2) and coupled-cluster theory with single and double excitations including perturbative corrections for the triple excitations (CCSD(T)) with various basis sets. The procedure involving determination of the CCSD(T)/6-31G(d) + CF level have been evaluated and applied to oxidation of several atmospheric hydrocarbons including isoprene, toluene, xylenes, pinenes.[37-47]

The topological analysis was performed using quantum theory of atoms in molecules (QTAIM) of Bader[35] with the AIM2000 package[48-50] at B3LYP/6-31G(d,p) level to investigate the nature of hydrogen-bonded complexes. We focused on the topological properties (e.g. charge density and its Laplacian, energy density) at hydrogen bond critical points (BCPs) to evaluate the strength of hydrogen bonding interactions between sulfuric acid, ammonia, water and organic acids.

3. Results and Discussion

3.1 Geometrical analysis

The geometries of H_2SO_4, H_2O, NH_3 and organic acids were optimized at the B3LYP/6-31G(d,p) level using the Gaussian 03 package.[36] The calculated structural parameters (e.g. bond length, bond angle) were found to be in good agreement with the available experimental data.

For sulfuric acid, we adopted the trans conformation. The equilibrium structures of those molecules were then employed to construct the relevant complexes and search for their global minima by considering all possible orientations. The DFT-B3LYP has proven to be appropriate by considering the trade offs between the computational accuracy and efficiency due to heavy organic acids used in this study. Several possible stable configurations of the complexes between sulfuric acid, organic acids and ammonia were found; however, we only report the most stable configuration, which bears a hydrogen bond pair in the complex, as will be discussed next.

Figures 1 and 2 depict the optimized geometries of the hydrogen bonded complexes of cis-pinonic acid, sulfuric acid and water, and the complexes of sulfuric acid, organic acids and ammonia at the B3LYP/6-31G(d,p) level, respectively. The investigated heteromolecular dimer complexes possess a hydrogen bond pair, which forms a 6- or 8-membered cyclic ring. The bonding strength of one hydrogen bond is stronger than that of the other. The hydrogen bonds of a trimer containing sulfuric acid, cis-pinonic acid, and/or water are characterized by the two hydrogen bond pairs connected by a molecule of sulfuric acid. The hydrogen bond (O-H•••X) (X = O or N) lies in the electron-deficient hydrogen and the high electron density of oxygen or nitrogen. The bond length of the hydrogen bonds ranges from 1.496 Å to 1.724 Å for the stronger bonding and from 1.708 Å to 2.383 Å for the weaker bonding, as shown in Table 1. For sulfuric acid monohydrate, one of the hydrogen bonds is much stronger than the other as indicated by their bond length (1.627 Å vs 2.094 Å). A similar characteristic feature was found in the sulfuric acid–ammonia complex; the bond length (1.550 Å) of the hydrogen bond (O-H•••N) is substantially shorter than that (2.383 Å) of the hydrogen bond (N-H•••O), indicating sulfuric acid as the hydrogen donor, water and ammonia as the hydrogen acceptor in both sulfuric acid monohydrate and sulfuric acid–ammonia complexes. The hydrogen bonds in the

organic acid–sulfuric acid complexes are comparable: one is slightly stronger than the other. For example, the stronger hydrogen bond has a bond length of 1.520 Å (1.503 Å) and the weaker hydrogen bond has a bond length of 1.705 Å (1.720 Å) for the cis-pinonic acid–sulfuric acid (benzoic acid–sulfuric acid) complex. For cis-pinonic acid–sulfuric acid complex, since there is still one electron-deficient hydrogen atom left in the sulfuric acid side, further addition of water, sulfuric acid or cis-pinonic acid results in the formation of a trimer, which generates another hydrogen bond pair, similar to the one mentioned above. The sulfuric acid molecule is located in the center of the trimer, shared by the two cyclic hydrogen-bonded rings. A pair of hydrogen-bonds with equivalent strength is formed in the homomolecular dimer of sulfuric acid, benzoic acid and cis-pinonic acid. For the organic acid–ammonia complexes, the stronger hydrogen bond (bond length: 1.70–1.72 Å) is weaker than the corresponding hydrogen bond in the sulfuric acid–ammonia complex and the bond length of the weaker hydrogen bond is comparable to that in the sulfuric acid–ammonia complex (2.24 to 2.31 vs 2.38 Å). Hence the interactions between organic acids and ammonia are likely weaker than those between sulfuric acid and ammonia.

The interactions between organic acids and sulfuric acid involve a category of homonuclear hydrogen bonds (-O-H•••O=) where two oxygen are interconnected by a system of π-conjugated double bonds, the so-called resonance-assisted hydrogen bonding (RAHB), which has been studied extensively over decades.[51-58] The contact distance d(O---O) between the two oxygen atoms in the hydrogen bond (-O-H•••O=) has been employed as an indicator of the hydrogen bond strength.[59] The distance d(O---O) < 2.5 Å is classified as very strong, 2.5 < d(O---O) <2.65 Å as strong, 2.65 < d(O---O) <2.80 Å as medium and d(O---O) > 2.8 Å as weak. As shown in Table 2, all the stronger hydrogen bonds of the pairs in the dimer and trimer fall into the strong hydrogen bond category as defined above with d(O---O) of 2.53–2.63 Å; all the

weaker hydrogen bonds in these complexes belong to the medium-strength hydrogen bond with d(O---O) of 2.66–2.72 Å. Another characteristic feature for this category of hydrogen bonding is the bond angles (-O-H•••O=) close to 180˚, and the cyclic ring connected by the hydrogen pair forms almost a plate, serving as a strong connection between two moieties. These results indicated that the molecular interactions between organic acid and sulfuric acid is via the formation of a hydrogen bond pair with one strong and one medium-strength of hydrogen bonding, which bears both electrostatic and covalent interaction in nature. The heteronuclear hydrogen bonds (O-H•••N and N-H•••O), formed in the complexes of organic acids and ammonia, are weaker than those in organic acid–sulfuric acid complexes. The hydrogen bond pairs in these organic acid–ammonia complexes are medium and weak hydrogen bonding and essentially electrostatic in nature.

Other structural modifications of the complexes upon formation of the hydrogen bonds can be evaluated from the lengthening or shortening of certain bonds adjacent to the hydrogen bonds (XO-H•••Y) (X = S or C and Y = O or N) or (Z-H•••O) (Z = N or O). For example, the O-H bond length in the cis-pinonic acid–sulfuric acid complex is increased by 0.02 and 0.06 Å for the stronger and the weaker hydrogen bond, respectively. Similarly, in the case of benzoic acid–ammonia complex, the O-H and N-H bond is elongated 0.04 and 0.01 Å, respectively. The lengthening or shorting of the O-H or N-H bond is explained by the balance between hyperconjugation and rehybrization. The hyperconjugative interaction (or charge transfer) from the lone pair of the hydrogen bond acceptor to the antibonding σ*(O-H or N-H) orbital of the hydrogen bond donor leads to the lengthening of the O-H or N-H bond; while the increase in s-character of the O-H or N-H bond due to the decrease of the effective electronegativity of hydrogen upon the formation of hydrogen bond result in the shortening of the N-H or O-H

bond.[56] The calculated lengthening of the N-H or O-H is a result of the balance of these two effects, with the hyperconjugation dominant over the rehybridization for all hydrogen-bonded complexes studied here. The domination of charge transfer on the lengthening of the N-H and O-H bond has been reflected in the charge distribution around the cyclic hydrogen bond ring structure. For example, the Mulliken charges (taken from frequency calculations) of the hydrogen atoms in the hydrogen bond pair are increased from 0.359 of sulfuric acid and 0.321 of cis-pinonic acid to 0.415 and 0.380 of the cis-pinonic acid–sulfuric acid complex, indicating a decrease in the effective electronegativity of hydrogen upon the hydrogen bond formation. Similar increases in the Mulliken charges of the hydrogen atoms in the investigated hydrogen-bonded complexes are also observed.

Lengthening or shortening of the above-mentioned bonds results in the red shift or blue shift of the stretching frequencies upon the formation of the hydrogen bond. Tables 3 and 4 depict the stretching frequencies of sulfuric acid, organic acid, and water complexes involving the red shift and blue shift and the corresponding frequencies of the monomers. For example, the lengthening of the SO-H and CO-H bonds in the cis-pinonic acid–sulfuric acid complex is 0.057 and 0.020 Å, respectively, resulting in red shifts of the corresponding stretching frequencies of 1066 and 391 cm^{-1}, respectively. For the same complex, the S=O and C=O bond lengths are increased by 0.019 and 0.023 Å, respectively, corresponding to a red shift of 295 and 105 cm^{-1}, respectively. The only blue shift of 59 cm^{-1} in the cis-pinonic acid–sulfuric acid complex exists for the S-OH bond, due to the shortening of ~ 0.052 Å for this bond. Table 5 shows a similar red shift of the stretching frequencies for N-H, CO-H and C=O bonds related to the hydrogen bonds of the organic acid–ammonia complexes. We calculated the absorption intensities of the monomers and the hydrogen bonded complexes and the distinct features of the corresponding IR

spectra were obtained. Figure 3 shows the calculated IR spectrum of the sulfuric acid (top), cis-pinonic acid–sulfuric acid complex (middle) and the cis-pinonic acid. The most intense absorption peaks are related to the vibrational stretching modes of the hydrogen bonds. The characteristic features of the calculated IR spectra of the organic acid–sulfuric acid complexes likely provide valuable information for the detection of these complexes in the atmosphere.

3.2 Thermochemical analysis

Relevant thermochemical parameters (e.g., binding energy, enthalpy, entropy, and Gibbs free energy) for the complex formation at 1 atm and 298K were calculated using various methods with different basis sets. The energy and other thermochemical data were taken from the Gaussian calculations and the above-mentioned thermochemical properties were computed according to the following formula,

$$\Delta_r E_B^o(298K) = \sum(\varepsilon_0 + ZPE)_{prod} - \sum(\varepsilon_0 + ZPE)_{react} \quad (1)$$

$$\Delta_r H^o(298K) = \sum(\varepsilon_0 + H_{corr})_{prod} - \sum(\varepsilon_0 + H_{corr})_{react} \quad (2)$$

$$\Delta_r G^o(298K) = \sum(\varepsilon_0 + G_{corr})_{prod} - \sum(\varepsilon_0 + G_{corr})_{react} \quad (3)$$

$$\Delta_r S^o(298K) = \frac{\Delta_r H^o(298K) - \Delta_r G^o(298K)}{298} \quad (4)$$

where $\Delta_r E_B^o(298K)$, $\Delta_r H^o(298K)$, $\Delta_r G^o(298K)$ and $\Delta_r S^o(298K)$ are binding energy, enthalpy, Gibbs free energy and entropy, respectively. ε_0, ZPE, H_{corr} and G_{corr} are the total energy at 0K, zero-point energy correction, thermal correction to enthalpy and thermal correction to Gibbs free energy, respectively. Tables 6 to 8 summarize the thermochemical parameters for the sulfuric acid, organic acid, ammonia and water complexes, computed using various methods with different basis sets at 298K and 1 atm. It is clear that the thermochemical parameters are strongly dependent on the methods and basis sets. In general B3LYP/6-31G(d,p) level predicts

the highest binding energies for the complex formation. The binding energies of ~20 kcal mol^{-1} are obtained for cis-pinonic acid–sulfuric acid and benzoic acid–sulfuric acid complexes, about 3–7 kcal mol^{-1} higher than those for organic acid–ammonia complexes at B3LYP/6-31G(d,p) level. Higher levels of theory (e.g., CCSD(T) and G2(MP2, SVP)) were also employed to calculate the binding energies of complex formation. Since the size of the cis-pinonic acid–sulfuric acid complex is large, higher level calculations (e.g. QCISD(T) and CCSD(T) level) were prohibitive, and only binding energies at B3LYP and PW91PW91 levels are reported for this complex. The binding energies at the two highest levels (G2(MP2, SVP) and CCSD(T) + CF) are in good agreement with each other (within 0.6 kcal mol^{-1}) for all the complexes presented in Tables 6–7. Binding energies of ~17.6, 8.5–9.5 kcal mol^{-1} at G2(MP2, SVP) and CCSD(T) + CF levels are obtained for the benzoic acid–sulfuric acid, organic acid–ammonia complexes, respectively. We estimated the binding energy of the same magnitude at both G2(MP2, SVP) and CCSD(T) + CF levels for cis-poninic acid–sulfuric acid complex. The higher binding energies for the organic acid–sulfuric acid than those for the organic acid–ammonia reflect stronger hydrogen bonding in organic acid–sulfuric acid complexes, which is consistent with the geometrical analysis. Binding energies of benzoic acid dimer and cis-pinonic acid dimer are 19.5 and 18.4 kcal mol^{-1}, respectively, in the same magnitude for the organic acid–sulfuric acid complexes. However, once formed, no more hydrogen acceptor or donor is available for further growth via hydrogen bonding interactions. Hence, homomolecular dimer formation contributes insignificantly to new particle formation. Addition of a third molecule (water, sulfuric acid or cis-pinonic acid) into the cis-pinonic acid–sulfuric acid can further stabilize the complex by ~13, 16, 18 kcal mol^{-1} at the B3LYP/6-31G(d, p) level, respectively. We carried out additional high levels of calculations. The binding energy is 8.1 (13.6) kcal mol^{-1} at B3LYP/6-

311++G(2d, 2f) level for addition of a water (sulfuric acid) molecule to the cis-poninic acid–sulfuric acid complex. The binding energies are 9.9 and 14.4 kcal mol^{-1} at PW91PW91/6-311++G(2d, 2f) level, respectively, for addition of a water and sulfuric acid molecule to the complex. The calculations for the poninic acid–sulfuric acid– poninic acid (PA-SA-PA) complex in both B3LYP/6-311++G(2d,2f) and PW91PW91/6-311++G(2d,2f) were problematic, and no binding energies at these two levels were reported for this complex.

The enthalpy of complex formation is also presented in Tables 6 to 8 and the values of the formation enthalpy are of the same magnitude (within 1 kcal mol^{-1}) as the corresponding binding energies for most of the complexes at various levels except for a few cases, for which the differences between binding energy and the formation enthalpy are ~ 3 kcal mol^{-1} (e.g., benzoic acid–sulfuric acid at B3LYP, CCSD(T) levels). The Gibbs free energies of the complex formation are also strongly dependent on the methods and the basis sets. The B3LYP/6-31G(d,p) level predicts higher values of Gibbs free energies. For example, the Gibbs free energies for formation of benzoic acid–sulfuric acid, cis-poninic acid–sulfuric acid are -8.8, -7.9 kcal mol^{-1}, respectively, while the Gibbs free energies for organic acid–ammonia formation fall in the range of -4.1 ~ -6.7 kcal mol^{-1}. The Gibbs free energies for benzoic acid–sulfuric acid are -7.6 and -6.6 at G2(MP2,SVP) and CCSD(T)+CF level, respectively. However, for organic acid–ammonia complexes, the Gibbs free energies are much less, in the range of 0 ~ -1 kcal mol^{-1} at the same levels. The values of the Gibbs free energies for the organic acid–sulfuric acid complexes are estimated to be several kcal mol^{-1} higher than those for the organic acid–ammonia complexes at the same levels, indicating that a larger thermodynamic stability for the organic acid–sulfuric acid complexes. Also, addition of a third molecule to the cis-poninic acid–sulfuric acid complex further stabilizes the complex by lowering the Gibbs free energies by 5.6 ~ 7.8 at B3LYP/6-

31G(d,p) level. Note that since the sizes of the organic acid–sulfuric acid complexes are large, the calculations are rather expensive and even prohibitive with current computation power.

3.3 Topological analysis

The bond length and binding energy can be used to evaluate the hydrogen bond strength, as discussed in previous sections. Topological properties (e.g., the electron density, Laplacian of the electron density and total energy density) of the hydrogen bonds provide alternative ways to study the hydrogen bond strength. According to Bader's theory of atoms in molecules,[35] the nuclei are defined as the attractors of the gradient vector field of charge distribution, which denote as (3, -3) critical points and have maxima of charge density. An atom is thus viewed as the union of an attractor (nuclear) and its associated basin (electron density distribution). An interatomic surface is defined as the boundary of the basin of the atom that has zero gradient of charge density.[60,61] All the gradient paths except two paths terminate at a point (denoting (3, -1) critical point) such that the Hessian matrix of the charge density at this point has two negative and one positive eigenvalues. The two paths originate from the bond critical point (3, -1) and terminate at neighboring attractors. These two paths form a line, the so-called bond path. A ring surface is defined as an infinite set of gradient paths which originate at a (3, +1) critical point where there are two positive and one negative eigenvalues of Hessian matrix of the charge density. In contrast, the ring paths originate at the adjacent bond critical point and terminate at the ring critical points (3, +1).[35] In this study, the electronic charge densities of the complexes and clusters were generated at the B3LYP/6-31G(d,p) level and the produced wave functions from DFT calculations were used as inputs of topological analysis. The bond and ring critical points of the electron densities of the complexes and clusters were then calculated and identified in the molecular graph as shown in Figures 4 and 5, along with the bond paths and the ring paths.

The arrows indicate the bond critical points (BCP) of the hydrogen bonds. The topological feature of the complexes is that there exists a nearly planar, 6- or 8-membered cyclic ring structure with a pair of hydrogen bonds and for each hydrogen bond, the BCP lies closely to the H nuclei. The bond paths connect the atoms in the ring and the Poincare-Hopf relation[35] hold for the relationship among the number of nuclei (N), bond critical point (N_{bcp}), ring critical point (N_{rcp}) and cage critical point (N_{ccp}): $N-N_{bcp}+N_{rcp}-N_{ccp} = 1$. The length of the bond path is not necessarily equal to the equilibrium bond length due to the curvature effect. However, the curvature effect on the hydrogen bonds in this study is insignificant; the bond path length (BPL) is very close to the corresponding equilibrium bond length (Re), except for H_2SO_4–H_2O and H_2SO_4–NH_3 complexes, as shown in Table 9. The ratio of BPL to Re is as high as 1.077 in the case of H_2SO_4–NH_3 and the bond path is inwardly curved toward the H nuclear in the weaker hydrogen bond of the pair. The ratio of the gradient path length from the BCP to O or N nuclear (r1) and from BCP to H (r2) in the hydrogen bond O(or N)•••H is correlated to the strength of the hydrogen bond. Figure 6 shows the ratio r1/r2 as a function of hydrogen bond path length (and hence the equilibrium hydrogen bond length). The ratio ranges from 2.0 to 2.4 for the bond length of 1.50–1.72 Å and decreases to 1.5–1.6 when the hydrogen bond length is increased to 2.1–2.4. The figure also shows the shorter the bond path length the higher the ratio, indicating the stronger the hydrogen bonds the higher the ratio (r1/r2). The curvature of the bond path in the molecular graph reflects the deviation of the configuration of the molecular structure to its equilibrium configuration of minimum energy.

Topological parameters (e.g. charge density and its Laplacian, the electronic kinetic, potential and total energies) at the bond critical points (BCPs) can be employed to evaluate the nature of hydrogen bonding interactions in the complexes. Koch and Popelier proposed eight

topological criteria based on the theory of atoms in molecules to characterize the types of the hydrogen bonds.[62] The closed-shell interactions (e.g., ionic bonds, hydrogen bonds and van der Waals interactions) correspond to a positive value of Laplacian of charge density at BCP, whereas for covalent bonds the Laplacian has a negative value. The strength of the hydrogen bonds correlates with the charge density and in general the larger for the value of the charge density, the stronger the hydrogen bond. The accumulation of the charge in the bonding region results in a decrease of the curvature of the charge density along the internuclear axis, providing an explanation of minor curvature of the strong hydrogen bonding as mentioned above. Two quantitative criteria have been suggested to characterize the hydrogen bond: the charge density and its Laplacian, in the range of 0.002–0.035 au and 0.024–0.139 au respectively.[59] As shown in Table 10, the value of charge density of the stronger hydrogen bond of the pair in this study ranges from 0.046 to 0.080 au and these values exceed the upper value of charge density proposed by Koch and Popelier.[62] Similarly, the Laplacian of charge density of the complexes composed of sulfuric acid, organic acid and water is in the range of 0.14–0.16 au, higher than the upper value of the Laplcian criteria. The high values of the charge density and Laplican strongly indicate that the hydrogen bonding interaction between sulfuric acid and organic acids is quite strong, consistent with the above-mentioned geometrical characterization of covalent bonding in nature for the stronger hydrogen bond of the pair. For the organic acid– sulfuric acid complexes, the weaker hydrogen bond of the pair is classified as medium strength as mentioned in the geometrical analysis, which can be seen from the values of the charge density and the Laplacian, in the range of 0.039–0.045 au and 0.12–0.14 au respectively. However, for sulfuric acid mono hydrate and ammonia–sulfuric acid (or organic acids) complexes, the hydrogen bond pair in these complexes is only in medium to low strength due to a generally-lower values of both

charge density and Laplacian of these hydrogen bonds at BCPs, which is also consistent with those from geometrical analysis. The bond ellipticity ($\epsilon = \lambda_1/\lambda_2-1$) ($\lambda_1$, $\lambda 2$ are the first two eigenvalues of the Hessian matrix) of the Hessian matrix provides another measure of not only charge accumulation in a given plane but also its structural stability. Substantial bond ellipticities correspond to structural instability, indicating that the bonding interaction is not strong and easily broken. The bond elliticities of the medium to weak hydrogen bonds are substantially greater than those of the strong hydrogen bonds in this study.

The electronic energy density K(r) can be used to characterize the bonding strength of the hydrogen bonds, and K(r) is related to the Laplacian of the charge density by a local expression of the virial theorem,[35]

$$\left(\frac{\hbar}{4m}\right)\nabla^2\rho(r) = K(r) + G(r) \tag{5}$$

where $K(r) = G(r) + V(r)$, G(r) is the electronic kinetic energy density, which is always positive, and V(r) is the electronic potential energy density, which is always negative. M and $\hbar$ are the mass of an electron and the Planck constant, respectively. As discussed above, a positive Laplacian at a BCP indicates that the hydrogen bonding interaction is dominated by the contraction of the charge away from the interatomic surface toward each nuclear and, hence, depletion of the charge along the bond path. For the hydrogen bonding interactions in this study, the Laplacian is found to be positive, indicating that the electronic kinetic energy density is in local excess over the magnitude of the corresponding total electronic energy density in the virial theorem, $G(r)>|K(r)|$ (or $2G(r)>|V(r)|$). In addition, for strong hydrogen bonding interaction, the total electronic energy density K(r) is found to be negative, showing partially covalent and partially electrostatic in nature; whereas this quantity is positive for medium and weak hydrogen bonds, revealing only electrostatic interactions for this bonding. As shown in Table 10, the

electronic energy density of the hydrogen bond 1 and 3 is negative except for that of the dimer of sulfuric acid, and the values of the K(r) of the sulfuric acid–organic acid complexes at BCPs is generally higher than those of the organic acid–ammonia complexes. Interestingly, the electronic energy densities of the sulfuric acid-ammonia (SA-AM) are found to be the highest. For hydrogen bonds 2 and 4, however, the electronic energy densities of these hydrogen bonds at BCPs are positive or slightly negative, revealing weaker interactions for these hydrogen bonds.

4. Conclusions

Formation of molecular complexes and clusters of potential atmospheric aerosol nucleation precursors were investigated by theoretical methods. We performed quantum chemical calculations to explore the structures, energetics and topology of complexes from sulfuric acid, organic acid, ammonia and water. Geometrical analysis shows that organic acid–sulfuric acid complexes bear a hydrogen bond pair with one strong and one medium-strength hydrogen bonding, while for organic acid–ammonia complexes the corresponding hydrogen bond pair is much weaker. The binding energies for organic acid–sulfuric acid complexes are also higher than those for organic acid–ammonia complexes by several kcal mol^{-1}. Topological analysis employing quantum theory of atoms in molecules (QTAIM) shows that the charge density and the Laplacian at BCPs of the hydrogen bonds of the organic acid–sulfuric acid are positive and falls in the range or exceeds the range of one strong and one medium-strength hydrogen bonding criteria. In the atmosphere, due to the abundance of the organic acids, strong hydrogen-bonding interactions between organic acid and sulfuric acid provide a driving force for the formation of organic acid-sulfuric acid complex, which is likely responsible for a reduction of nucleation barrier by modifying the hydrophobic properties of organic acid and allowing further addition of hydrophilic species (e.g., H_2SO_4, H_2O, and possible NH_3) to the hydrophilic

side of the clusters, propelling the nascent growth of the new particles. This study provides the geometrical, energetical and topological information of hydrogen-bonding interactions in the atmospheric complexes and helps to elucidate the structure, size, composition and other properties of atmospheric clusters, bridging the gap between the molecule and the newly-formed nuclei.

Acknowledgment

This work was supported by the Robert A. Welch Foundation (Grant A-1417). Additional support was provided by the Texas A&M University Supercomputing Facilities. The authors acknowledged the use of the Laboratory for Molecular Simulations at Texas A&M and Dr. Lisa M. Pérez for assistance with the calculations.

References

(1) Kanakidou, M.; Seinfeld, J. H.; Pandis, S. N.; Barnes, I.; Dentener, F. J.; Facchini, M. C.; Van Dingenen, R.; Ervens, B.; Nenes, A.; Nielsen, C. J.; Swietlicki, E.; Putaud, J. P.; Balkanski, Y.; Fuzzi, S.; Horth, J.; Moortgat, G. K.; Winterhalter, R.; Myhre, C. E. L.; Tsigaridis, K.; Vignati, E.; Stephanou, E. G.; Wilson, J. *Atmos. Chem. Phys.* **2005**, *5*, 1053.

(2) Kulmala, M.; Vehkamaki, H.; Petajda, T.; Dal Maso, M.; Lauri, A.; Kerminen, V. M.; Birmili, W.; McMurry, P. H. *J. Aerosol Sci* **2004**, *35*, 143.

(3) McMurry, P. H; Fink, M.; Sakurai, H.; Stolzenburg, M.R.; Mauldin, R.L.; Smith, J.; Eisele, F.; Moore, K.; Sjostedt, S.; Tanner, D.; Huey, L.G.; Nowak, J.B.; Edgerton, E.; Voisin, D. *J. Geophys. Res*. **2005**, *110*, D22S02, doi:10.1029/2005JD005901.

(4) Kim, T. O.; Ishida, T.; Adachi, M.; Okuyama, K.; Seinfeld, J. H. *Aerosol Sci. Technol.* **1998**, *29*, 111.

(5) Ball, S. M.; Hanson, D. R.; Eisele, F. L.; McMurry, P. H. *J. Geophys. Res.-Atmos* **1999**, *104*, 23709.

(6) Coffman, D. J.; Hegg, D. A. *J. Geophys. Res.-Atmos* **1995**, *100*, 7147.

(7) Korhonen, P.; Kulmala, M.; Laaksonen, A.; Viisanen, Y.; McGraw, R.; Seinfeld, J. H. *J. Geophys. Res.-Atmos* **1999**, *104*, 26349.

(8) Napari, I.; Kulmala, M.; Vehkamaki, H. *J. Chem. Phys.* **2002**, *117*, 8418.

(9) Napari, I.; Noppel, M.; Vehkamaki, H.; Kulmala, M. *J. Chem. Phys.* **2002**, *116*, 4221.

(10) Hanson, D. R.; Eisele, F. L. *J. Geophys. Res.-Atmos* **2002**, *107*.

(11) Zhang, R. Y.; Suh, I.; Zhao, J.; Zhang, D.; Fortner, E. C.; Tie, X. X.; Molina, L. T.; Molina, M. J. *Science* **2004**, *304*, 1487.

(12) Zhang, R.; Wooldridge, P.J.; Abbatt, J.P.D.; Molina M.J., *J. Phys. Chem.* **1993**, *97*, 7351.

(13) Zhang, R.; Wooldridge, P.J.; Molina, M.J. *J. Phys. Chem.* **1993**, *97*, 8541.

(14) Kurdi, L.; Kochanski, E. *Chem. Phys. Lett.* **1989**, *158*, 111.

(15) Arstila, H.; Laasonen, K.; Laaksonen, A. *J. Chem. Phys.* **1998**, *108*, 1031.

(16) Bandy, A. R.; Ianni, J. C. *J. Phys. Chem. A* **1998**, *102*, 6533.

(17) Re, S.; Osamura, Y.; Morokuma, K. *J. Phys. Chem. A* **1999**, *103*, 3535.

(18) Ding, C. G.; Laasonen, K.; Laaksonen, A. *J. Phys. Chem. A* **2003**, *107*, 8648.

(19) Ding, C. G.; Laasonen, K. *Chem. Phys. Lett.* **2004**, *390*, 307.

(20) Ianni, J. C.; Bandy, A. R. *J.Mol. Struct. -Theochem* **2000**, *497*, 19.

(21) Al Natsheh, A.; Nadykto, A. B.; Mikkelsen, K. V.; Yu, F. Q.; Ruuskanen, J. *J. Phys. Chem. A* **2004**, *108*, 8914.

(22) Kurten, T.; Sundberg, M. R.; Vehkamaki, H.; Noppel, M.; Blomqvist, J.; Kulmala, M. *J. Phys. Chem. A* **2006**, 110, 7178.

(23) Ianni, J. C.; Bandy, A. R. *J. Phys. Chem. A* **1999**, *103*, 2801.

(24) Larson, L. J.; Largent, A.; Tao F. M. Structure of the sulfuric acid-ammonia system and the effect of water molecules in the gas phase, *J. Phys. Chem. A* **1999**, 103, 6786.

(25) Kurten, T.; Torpo, L.; Ding, C. G.; Vehkamaki, H.; Sundberg, M. R.; Laasonen, K.; Kulmala, M. *J. Geophys. Res.-Atmos* **2007**, *112*. D04210, doi:10.1029/2006JD007391

(26) Emmeluth, C.; Suhm, M. A. *PCCP* **2003**, *5*, 3094.

(27) Nandi, C. K.; Hazra, M. K.; Chakraborty, T. *J. Chem. Phys.* **2005**, *123*.

(28) Sloth, M.; Bilde, M.; Mikkelsen, K. V. *Mol. Phys.* **2004**, *102*, 2361.

(29) Gora, R. W.; Grabowski, S. J.; Leszczynski, J. *J. Phys. Chem. A* **2005**, *109*, 6397.

(30) Nadykto, A. B.; Yu, F. Q. *Chem. Phys. Lett.* **2007**, *435*, 14.

(31) Koch, S.; Winterhalter, R.; Uherek, E.; Kolloff, A.; Neeb, P.; Moortgat, G. K. *Atmos. Environ.* **2000**, *34*, 4031.
(32) Capouet, M.; Muller, J. F. *Atmos. Chem. Phys.* **2006**, *6*, 1455.
(33) Fan, J.; Zhang, R.; Collins, D.; Li, G. *Geophys. Res. Lett*. **2006**, *33*, L15802, doi:10.1029/2006GL026295.
(34) McGraw, R.; Zhang, R. *J. Chem. Phys.* **2008**, *128*, 064508, DOI:10.1063/1.2830030.
(35) Bader, R. F. W. *Atoms in molecules: a quantum theory*; Clarendon Press: Oxford ; New York, 1990.
(36) Frisch, M. J.; Trucks, G. W.; Schlegel, H. B.; Scuseria, G. E.; Robb, M. A.; Cheeseman, J. R.;Montgomery, J. A. Jr. ; Vreven, T.; Kudin, K. N.; Burant, J. C.; Millam, J. M.; Iyengar, S. S.; Tomasi, J.; Barone, V.; Mennucci, B.; Cossi, M.; Scalmani, G.; Rega, N.; Petersson, G. A.; Nakatsuji, H.; Hada, M.; Ehara, M.; Toyota, K.; Fukuda, R.; Hasegawa, J.; Ishida, M.; Nakajima, T.; Honda, Y.; Kitao, O.; Nakai, H.; Klene, M.; Li, X.; Knox, J. E.; Hratchian, H. P.; Cross, J. B.; Adamo, C.; Jaramillo, J.; Gomperts, R.; Stratmann, R. E.; Yazyev, O.; Austin, A. J.; Cammi, R.; Pomelli, C.; Ochterski, J. W.; Ayala, P. Y.; Morokuma, K.; Voth, G. A.; Salvador, P.; Dannenberg, J. J.; Zakrzewski, V. G.; apprich, S.; Daniels, A. D.; Strain, M. C.; Farkas, O.; Malick, D. K.; Rabuck, A. D.; Raghavachari, K.; Foresman, J. B.; Ortiz, J. V.; Cui, Q.; Baboul, A. G.; Clifford, S.; Cioslowski, J.; Stefanov, B. B.; Liu, G.; Liashenko, A.; Piskorz, P.; Komaromi, I.; Martin, R. L.; Fox, D. J.; Keith, T.; Al-Laham, M. A.; Peng, C. Y.; Nanayakkara, A.; Challacombe, M.; Gill, P. M. W.; Johnson, B.; Chen, W.; Wong, M. W.; Gonzalez, C.; and Pople, J. A. Gaussian 03, Revision B.05, Gaussian, Inc., Pittsburgh PA, 2003.
(37) Lei, W. F.; Derecskei-Kovacs, A.; Zhang, R. Y. *J. Chem. Phys.* **2000**, *113*, 5354.
(38) Lei, W. F.; Zhang, R. Y. *J. Chem. Phys.* **2000**, *113*, 153.
(39) Suh, I.; Lei, W. F.; Zhang, R. Y. *J. Phys. Chem. A* **2001**, *105*, 6471.
(40) Suh, I.; Zhang, D.; Zhang, R. Y.; Molina, L. T.; Molina, M. J. *Chem. Phys. Lett.* **2002**, *364*, 454.
(41) Zhang, D.; Zhang, R. Y. *J. Am. Chem. Soc.* **2002**, *124*, 2692.
(42) Suh, I.; Zhang, R. Y.; Molina, L. T.; Molina, M. J. *J. Am. Chem. Soc.* **2003**, *125*, 12655.
(43) Suh, I.; Zhang, R. Y.; Molina, L. T.; Molina, M. J. *J. Am. Chem. Soc.* **2003**, *125*, 12655.
(44) Zhang, D.; Zhang, R. *J. Chem. Phys.* **2005**, *122*.
(44) Suh, I.; Zhao, J.; Zhang, R. Y. *Chem. Phys. Lett.* **2006**, *432*, 313.
(46) Fan, J. W.; Zhao, J.; Zhang, R. Y. *Chem. Phys. Lett.* **2005**, *411*, 1.
(47) Fan, J. W.; Zhang, R. Y. *J. Phys. Chem. A* **2006**, *110*, 7728.
(48) Biegler-Konig, F. *J. Comput. Chem.* **2000**, *21*, 1040.
(49) Biegler-Konig, F.; Schonbohm, J.; Bayles, D. *J. Comput. Chem.* **2001**, *22*, 545.
(50) Biegler-Konig, F.; Schonbohm, J. *J. Comput. Chem.* **2002**, *23*, 1489.
(51) Kollman, P. A.; Allen, L. C. *Chem. Rev.* **1972**, *72*, 283.
(52) Reed, A. E.; Curtiss, L. A.; Weinhold, F. *Chem. Rev.* **1988**, *88*, 899.
(53) Curtiss, L. A.; Blander, M. *Chem. Rev.* **1988**, *88*, 827.
(54) Gilli, P.; Bertolasi, V.; Ferretti, V.; Gilli, G. *J. Am. Chem. Soc.* **1994**, *116*, 909.
(55) Fiacco, D. L.; Hunt, S. W.; Leopold, K. R. *J. Am. Chem. Soc.* **2002**, *124*, 4504.
(56) Alabugin, I. V.; Manoharan, M.; Peabody, S.; Weinhold, F. *J. Am. Chem. Soc.* **2003**, *125*, 5973.
(57) Gilli, P.; Bertolasi, V.; Pretto, L.; Gilli, G. *J. Mol. Struct.* **2006**, *790*, 40.
(58) Pakiari, A. H.; Eskandari, K. *J.Mol. Struct. -Theochem* **2006**, *759*, 51.
(59) Ochterski, J. W. (2000), Thermochemistry in Gaussian, Gaussian Inc. Wallingford, CT.
(60) Bieglerkonig, F. W.; Bader, R. F. W.; Tang, T. H. *J. Comput. Chem.* **1982**, *3*, 317.
(61) Bader, R. F. W.; Tang, T. H.; Tal, Y.; Bieglerkonig, F. W. *J. Am. Chem. Soc.* **1982**, *104*, 946.

(62) Koch, U.; Popelier, P. L. A. *J. Phys. Chem.* **1995**, *99*, 9747.
(63) Popelier, P. L. A. *J. Phys. Chem. A* **1998**, *102*, 1873.

Table 1. Bond Length (in Angstrom) and Bond Angle (in degree) of the Hydrogen Bonds in the Complexes of Sulfuric Acid, Organic Acid, Ammonia and Water.

complex[a]	Hydrogen Bond 1[b]		Hydrogen Bond 2[c]	
	r(H···O(or N)	α(O-H···O or N)	r(H···O)	α(N or O-H···O)
W-SA	1.627	164.7	2.094	130.2
BA-SA	1.503	177.13	1.705	178.5
PA-SA	1.520	177.1	1.720	178.0
SA-SA	1.653	175.6	1.653	175.6
BA-BA	1.616	178.7	1.616	178.7
PA-PA	1.640	179.1	1.640	179.1
SA-AM	1.550	171.9	2.383	117.8
FA-AM	1.701	165.8	2.308	123.7
AA-AM	1.724	165.3	2.238	126.5
BA-AM	1.703	166.5	2.256	125.1
PA-SA-W	1.541	177.5	1.708	178.1
PA-SA-SA	1.496	178.1	1.730	178.3
PA-SA-PA	1.534	178.1	1.714	178.3
	Hydrogen Bond 3[a]		Hydrogen Bond 4[b]	
PA-SA-W	1.592	163.2	2.089	131.5
PA-SA-SA	1.632	178.3	1.665	178.1
PA-SA-PA	1.535	178.1	1.713	178.2

[a] W-SA: water-sulfuric acid complex; BA-SA: benzoic acid-sulfuric acid complex; PA-SA: cis-pinonic acid-sulfuric acid complex; SA-SA: sulfuric acid dimer; BA-BA: benzoic acid dimer; PA-PA: cis-pinonic acid dimer; PIA-NA: pinic acid-norpinic acid complex.
[b] Hydrogen bond with shorter bond length r(H···O) and α(O-H···O) is the bond angle.
[c] Hydrogen bond with longer bond length.

Table 2. Contact Distance d(O---O) (in Angstrom) of the Hydrogen Bond (-O-H•••O=) in the Organic Acid–Sulfuric Acid Complexes and Their Homomolecular Dimers.

Complex	HB pair 1		HB pair 2	
BA-SA	2.536	2.698		
PA-SA	2.549	2.712		
PA-SA-W	2.565	2.702	2.625	2.831
PA-SA-SA	2.532	2.720	2.635	2.660
PA-SA-PA	2.560	2.707	2.561	2.706
SA-SA	2.652	2.652		
BA-BA	2.624	2.624		
PA-PA	2.646	2.646		

Table 3. The Calculated Stretching Frequencies (in cm^{-1}) of Homomolecular Dimers of Sulfuric Acid and Organic Acid and Their Monomers.

Assig.	SA	W	BA	PA	SA-SA	BA-BA	PA-PA
CO-H			3767	3751		3091	3146
C=O			1819	1841		1759	1779
SO-H	3761				3252		
S=O	1437				1402		
S-OH	847				913		
HO-H		3911					

Table 4. The Calculated Stretching Frequencies (in cm^{-1}) of Sulfuric Acid/Organic Acid/Water Complexes.

Assig.	SA-W	BA-SA	PA-SA	PA-SA-W	PA-SA-SA	PA-SA-PA
CO-H		3346	3360	3337	3384	3328
C=O		1717	1736	1740	1730	1736
SO-H	3005	2620	2695	3044(2775)*	3129(2579)*	2723
S=O	1169	1139	1140	1142	1254(1124)*	1279
S-OH	890	928	906	841	908(855)**	965
HO-H	3867			3865		

* Values in parentheses are the bond stretching frequencies in PA side
** Value in parentheses is the bond stretching frequencies in center SA

Table 5. The Calculated Stretching Frequencies (in cm^{-1}) of Organic Acid/Ammonia Complexes.

Assig.	AM	SA-AM	FA-AM	AA-AM	BA-AM
CO-H			2921	3010	2959
C=O			1806	1804	1776
N-H	3587	3598	3589	3617	3587
SO-H		2314			
S=O		1369			
S-OH		915			

Table 6. Thermochemical Parameters for the Complex Formation at G2(MP2, SVP) Level.[a]

molecule	MP2(full)/ 6-31G(d,p)				QCISD(T)/ 6-31G(d)			G2(MP2, SVP)		
	BE	ΔH	ΔS	ΔG	BE	ΔH	ΔG	BE	ΔH	ΔG
BA_SA	16.47	-16.16	-150.43	-5.48	18.63	-18.37	-7.62	17.84	-18.30	-7.55
BA_AM	8.43	-9.54	-132.79	-0.11	12.02	-13.00	-3.57	9.43	-10.41	-0.98
AA_AM	8.13	-8.50	-126.49	0.48	11.41	-11.55	-2.57	8.85	-8.99	-0.01
FA_AM	8.61	-9.12	-126.46	-0.15	11.63	-11.91	-2.93	9.18	-9.46	-0.48

[a] BE (binding energy), ΔH (enthalpy of formation) and ΔG (Gibbs free energy of formation) are in kcal mol^{-1}; ΔS (entropy of formation) is in J mol^{-1} K^{-1}.

Table 7. Thermochemical Parameters for the Complex Formation at CCSD(T) + CF Level.

complex	B3LYP/ 6-31G(d,p)				CCSD(T)/ 6-31G(d)			CCSD(T)+CF		
	BE	ΔH	ΔS	ΔG	BE	ΔH	ΔG	BE	ΔH	ΔG
BA_SA	19.85	-23.18	-202.88	-8.78	18.23	-21.56	-7.16	17.62	-20.95	-6.55
PA_SA	19.20	-19.17	-158.75	-7.90						
BA_AM	12.80	-16.63	-176.02	-4.08	12.08	-15.91	-3.36	9.27	-13.09	-0.54
AA_AM	15.34	-15.86	-128.64	-6.69	11.45	-11.97	-2.80	8.45	-8.97	0.20
FA_AM	13.08	-13.73	-127.97	-4.61	11.88	-12.53	-3.40	8.73	-9.38	-0.26

Table 8. Thermochemical Parameters for the Complex Formation at B3LYP and PW91PW91 Level.

complex	B3LYP/ 6-31G(d,p)				B3LYP/ 6-311++G(2d,2p)			PW91PW91/ 6-311++G(2d,2p)		
	BE	ΔH	ΔS	ΔG	BE	ΔH	ΔG	BE	ΔH	ΔG
BA_SA_W	14.12	-14.92	-130.94	-5.59	8.14	-8.94	0.39	9.90	-10.71	-1.37
PA_SA_SA	17.16	-17.19	-149.27	-6.55	13.55	-13.58	-2.94	14.39	-14.43	-3.79
PA_SA_PA	19.03	-18.95	-156.94	-7.76						

Table 9. Comparison of the Equilibrium Bond Length and the Bond Path Length of the Complexes

Species	Hydrogen bond 1					Hydrogen bond 2				
	Re [a]	r1(Å)[b]	r2(Å)[b]	r1/r2	BPL	Re	r1(Å)	r2(Å)	r1/r2	BPL
SA-W	1.627	1.112	0.516	2.155	1.628	2.094	1.304	0.802	1.625	2.106
SA-AM	1.55	1.092	0.457	2.390	1.549	2.238	1.426	0.985	1.448	2.411
SA-SA	1.653	1.112	0.542	2.052	1.654					
BA-BA	1.617	1.101	0.516	2.136	1.617					
PA-PA	1.641	1.113	0.528	2.106	1.641					
BA-SA	1.503	1.047	0.457	2.290	1.504	1.705	1.139	0.568	2.006	1.707
PA-SA	1.52	1.055	0.466	2.263	1.521	1.72	1.146	0.576	1.989	1.722
AA-AM	1.724	1.179	0.545	2.163	1.724	2.238	1.368	0.878	1.559	2.246
BA-AM	1.703	1.169	0.534	2.188	1.703	2.256	1.376	0.890	1.545	2.266
FA-AM	1.701	1.168	0.533	2.189	1.701	2.308	1.400	0.918	1.525	2.318

[a] Re is the equilibrium bond length in Angstrom.

[b] r1, r2 is the length of gradient path from bond critical point (BCP) to O or N nuclear and from BCP to H nuclear, respectively.

Table 10. Topological Parameters (Charge Densities, Laplacian, Kinetic Energy Densities, Potential Energy Densities and Total Energy Densities) at BCPs of the Hydrogen Bonds of the Complexes. (unit in au)

Species	Hydrogen bond 1					Hydrogen bond 2				
	ρ (-2)	$\nabla^2 \rho$ (-2)	G(r) (-2)	V(r) (-2)	K(r) (-2)	ρ (-2)	$\nabla^2 \rho$ (-2)	G(r) (-2)	V(r) (-2)	K(r) (-2)
SA-W	5.53	14.44	4.02	-4.43	-0.41	2.02	6.37	1.63	-1.66	-0.03
	4.64	12.11	3.49	-3.95	-0.46	1.48	5.43	1.20	-1.04	0.16
SA-AM	7.96	8.88	4.65	-7.08	-2.43	1.24	4.46	1.02	-0.93	0.09
SA-SA	4.58	14.07	3.51	-3.50	0.01					
BA-BA	5.42	14.77	3.98	-4.28	-0.29					
PA-PA	5.11	14.16	3.73	-3.93	-0.19					
BA-SA	7.20	15.61	5.31	-6.72	-1.41	4.09	12.64	3.10	-3.04	0.06
PA-SA	6.87	15.71	5.07	-6.21	-1.14	3.96	12.19	2.98	-2.92	0.06
AA-AM	5.13	10.72	3.20	-3.71	-0.52	1.67	5.20	1.29	-1.28	0.01
BA-AM	5.38	10.95	3.35	-3.96	-0.61	1.61	5.12	1.26	-1.23	0.02
FA-AM	5.44	10.89	3.37	-4.01	-0.65	1.46	4.75	1.14	-1.10	0.04
PA-SA-W	6.49	15.73	4.80	-5.67	-0.87	4.08	12.52	3.08	-3.02	0.05
PA-SA-SA	7.35	15.36	5.38	-6.93	-1.54	3.87	11.91	2.91	-2.85	0.06
PA-SA-PA	6.63	15.66	4.88	-5.85	-0.97	4.03	12.37	3.04	-2.99	0.05
	Hydrogen bond 3					Hydrogen bond 4				
PA-SA-W	5.35	14.14	3.89	-4.24	-0.35	2.04	6.35	1.63	-1.67	-0.04
PA-SA-SA	4.87	14.60	3.72	-3.80	-0.08	4.47	13.72	3.41	-3.40	0.02
PA-SA-PA	6.60	15.73	4.87	-5.81	-0.94	4.04	12.37	3.04	-2.99	0.05

FIGURES CAPTIONS

Figure 1. The optimized geometries of the complexes of sulfuric acid, cis-pinonic acid and water at B3LYP/6-31G(d,p) level. (PA, SA, and W is cis-pinonic acid, sulfuric acid, and water, respectively).

Figure 2. The optimized geometries of the complexes of sulfuric acid, organic acids and ammonia at B3LYP/6-31G(d,p) level.

Figure 3. The calculated vibrational frequencies and the corresponding absorption intensities of cis-pinonic acid – sulfuric acid complex and its monomers.

Figure 4. Molecular graphs of the organic acid–sulfuric acid complexes showing the BCPs, ring critical points, bond path and ring path.

Figure 5. Molecular graphs of the sulfuric acid–water, sulfuric acid–ammonia and benzoic acid–ammonia complexes showing the BCPs, ring critical points, bond path and ring path.

Figure 6. Plot of r1/r2 as a function of equilibrium bond length.

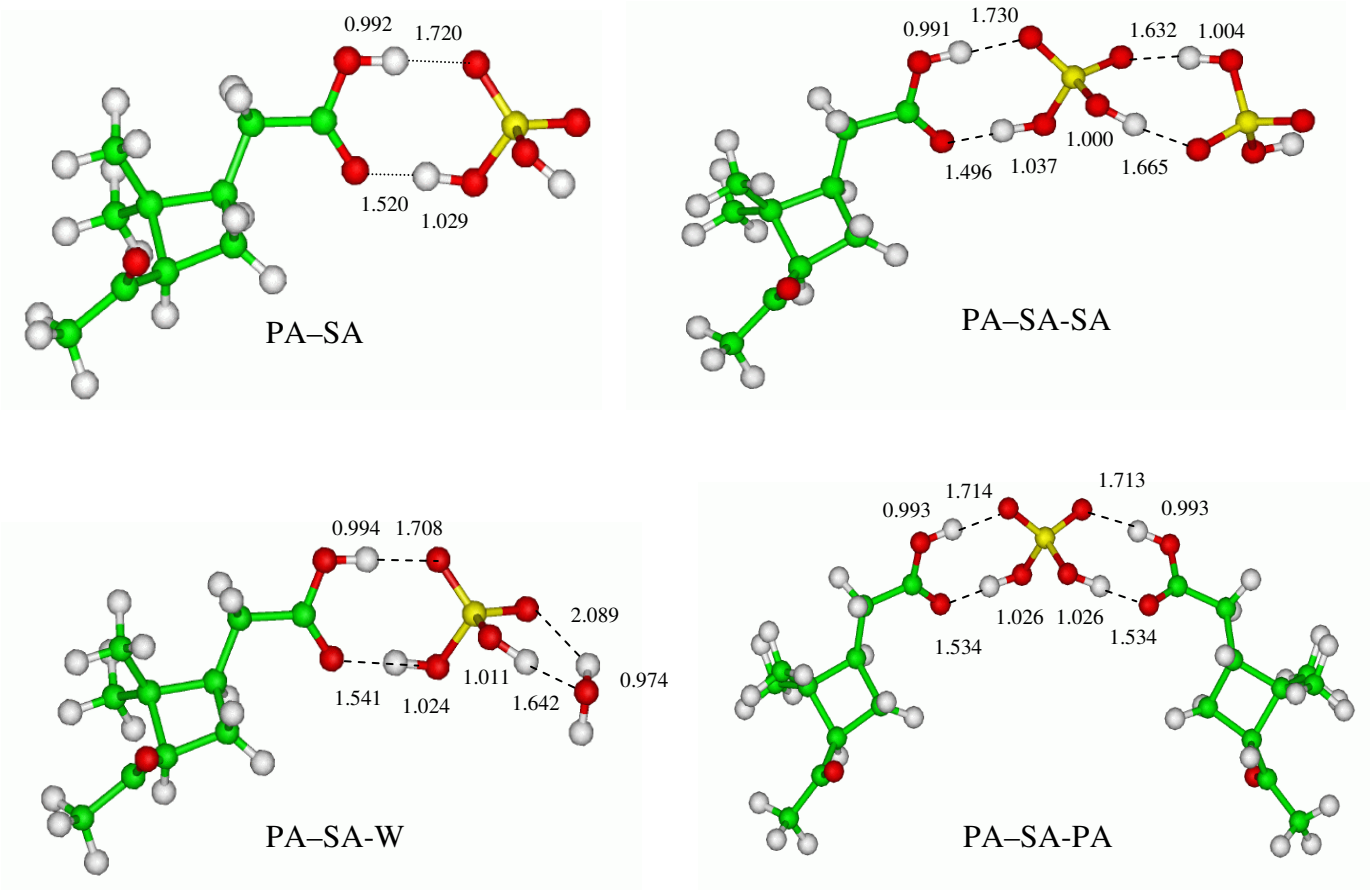
0.992
1.720
1.520
1.029
PA–SA
0.991
1.730
1.632
1.004
1.000
1.496
1.037
1.665
PA–SA-SA
0.994
1.708
2.089
1.011
0.974
1.541
1.024
1.642
PA–SA-W
0.993
1.714
1.713
0.993
1.026
1.026
1.534
1.534
PA–SA-PA

Figure 1.

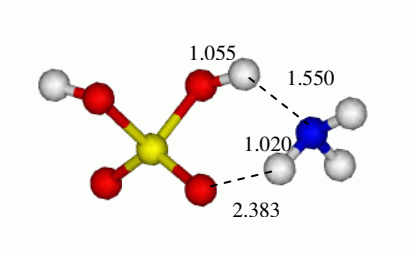

H_2SO_4–NH_3

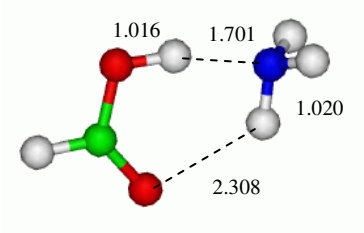

Formic acid–NH_3

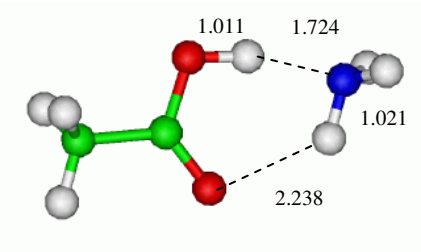

Acetic acid–NH_3

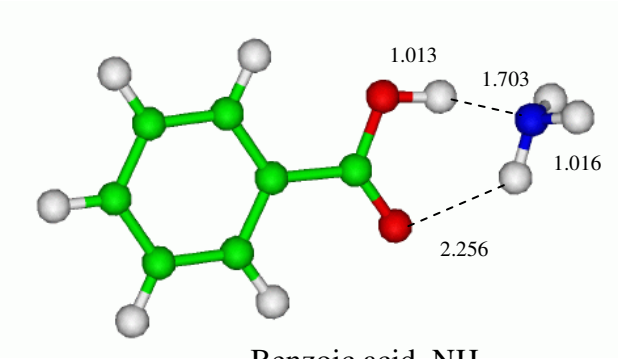

Benzoic acid–NH_3

Figure 2.

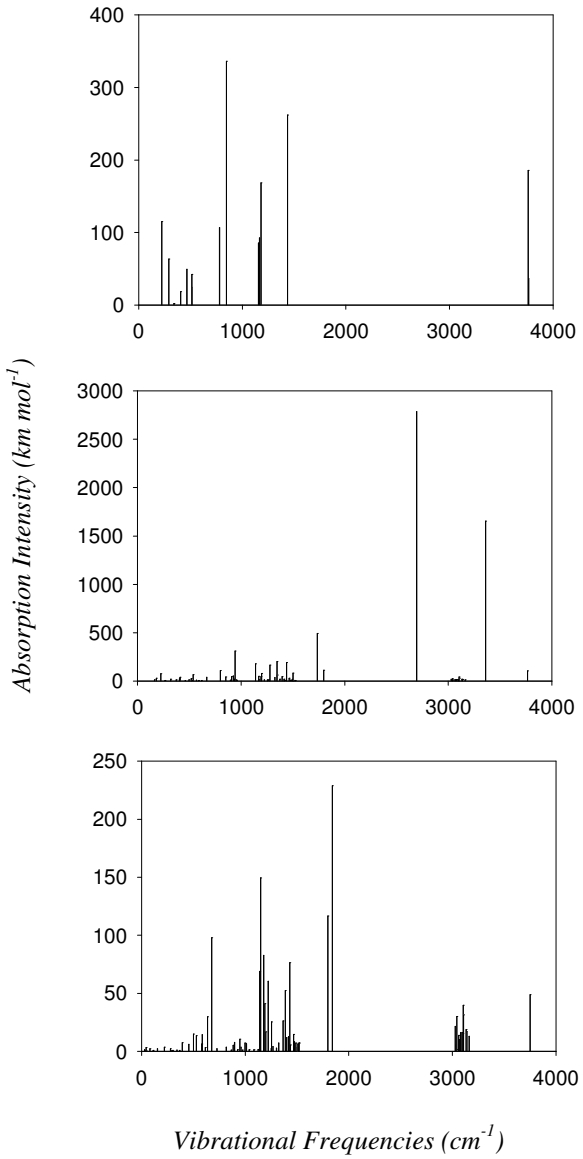
Absorption Intensity (km mol-1)
Vibrational Frequencies (cm-1)
400
300
200
100
0
0
1000
2000
3000
4000
3000
2500
2000
1500
1000
500
0
0
1000
2000
3000
4000
250
200
150
100
50
0
0
1000
2000
3000
4000

Figure 3.

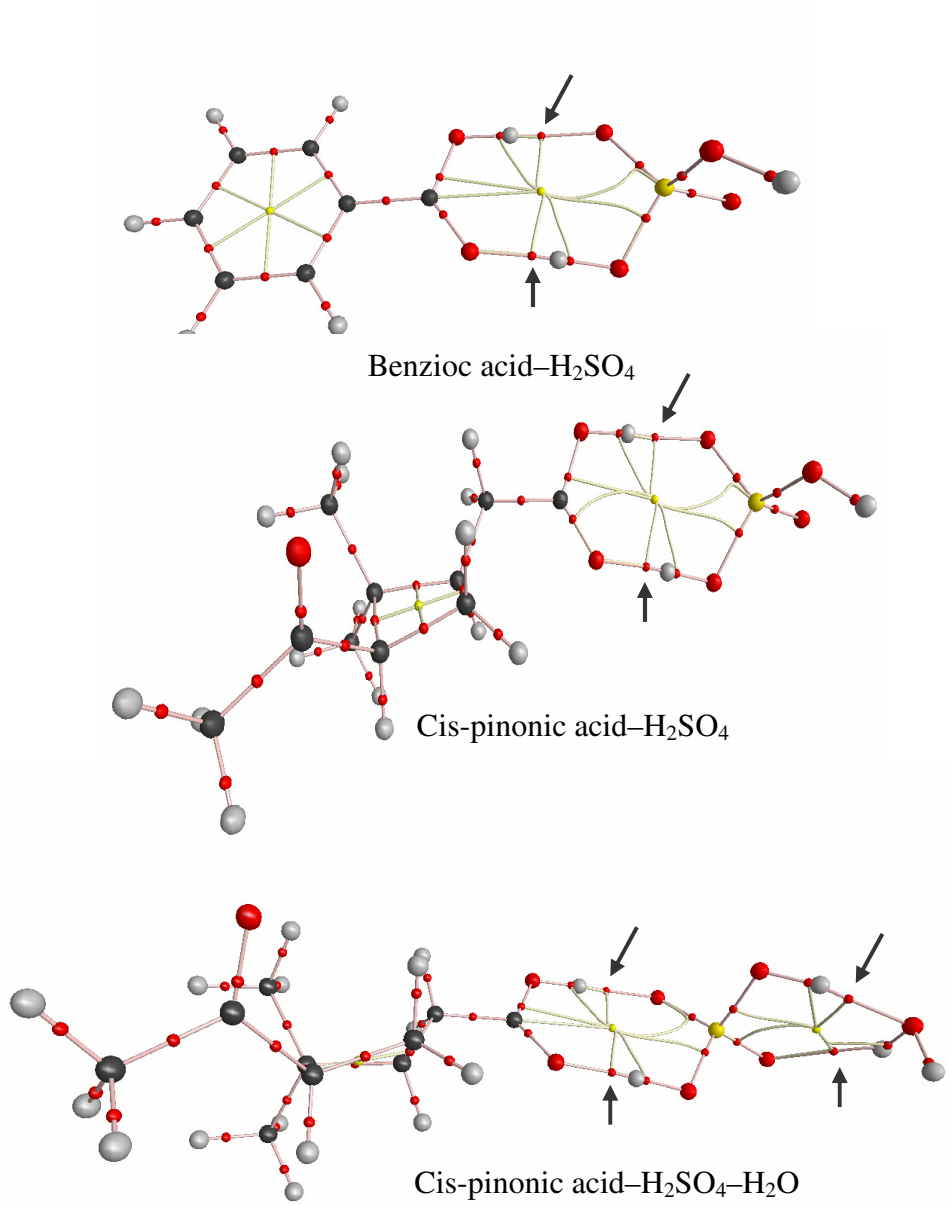
Benzioc acid–H_2SO_4
Cis-pinonic acid–H_2SO_4
Cis-pinonic acid–H_2SO_4–H_2O

Figure 4.

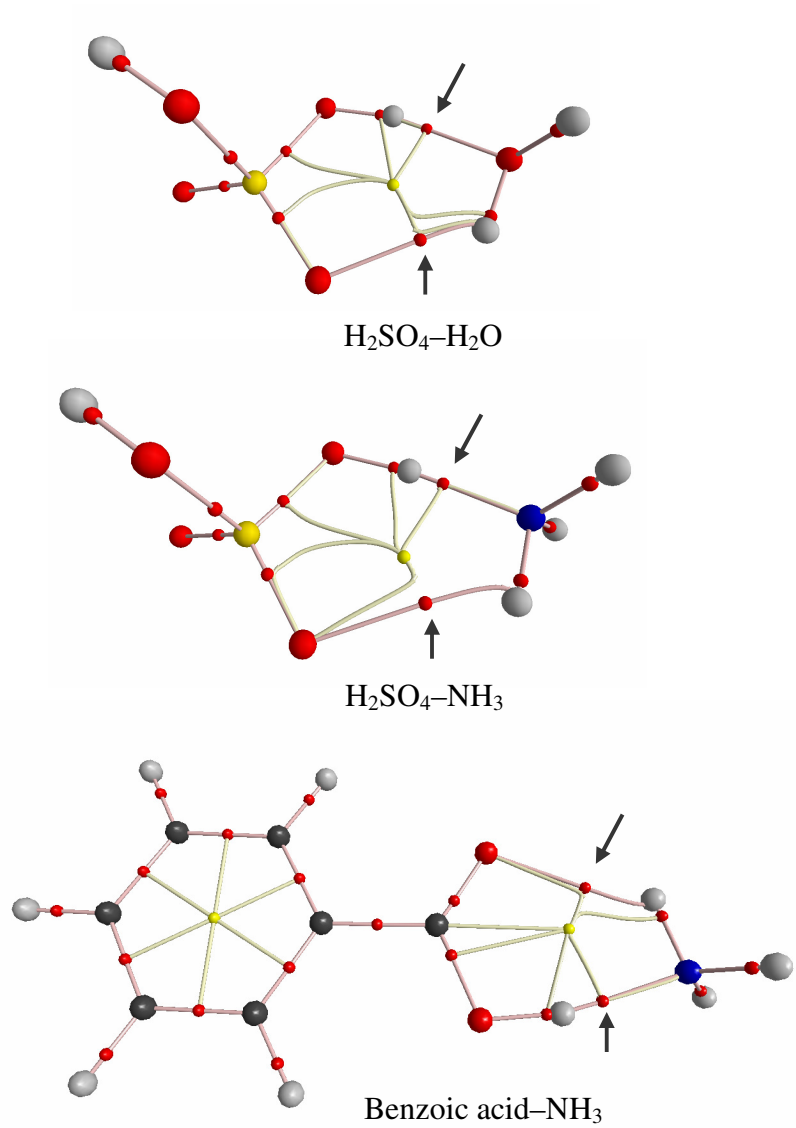

Figure 5.

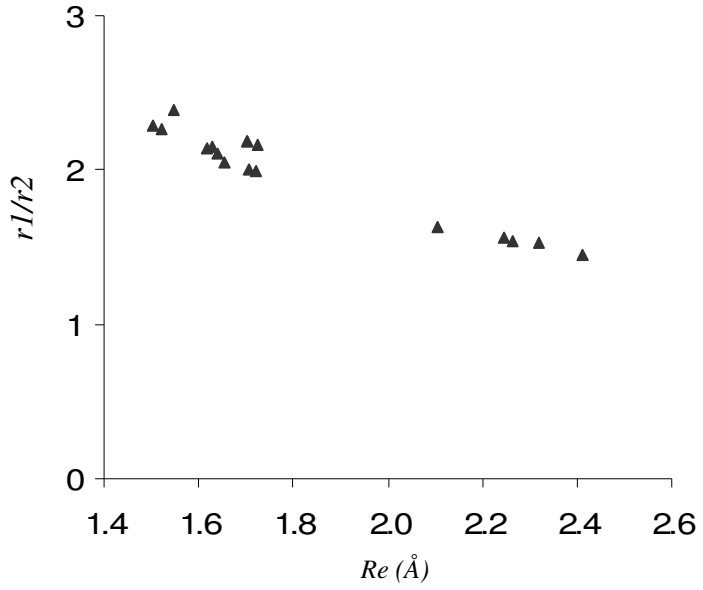

Figure 6.